Acta Astronautica 193 (2022) 370–380

Contents lists available at ScienceDirect

Acta Astronautica

journal homepage: www.elsevier.com/locate/actaastro

Research paper

Non-cooperative differential game based output feedback control for spacecraft attitude regulation

Xiaoyu Lang, Anton de Ruiter *

Ryerson University, Toronto, Ontario, M5B 2K3, Canada

ARTICLE INFO

Keywords:
Output feedback
Spacecraft attitude control
Linear differential game
Gain-scheduled control
Passivity

ABSTRACT

Retired spacecraft attitude takeover control using two types of cellular space modules, namely orientation cellular space module (OCSM) and rate cellular space module (RCSM), is considered in this paper. Both the OCSM and the RCSM are endowed with identical mechanical actuators for providing 3-axis torques for attitude regulation. The difference is: the OCSM is equipped with orientation sensors which provide unit-length vector measurements to determine attitude, while the RCSM is mounted with rate sensors which measure angular velocities. Correspondingly, the attitude takeover controller is composed of a pre-wrap proportional control part and an output (angular velocity) feedback control part, which are executed by the OCSM and the RCSM respectively. A gain-scheduled control framework is adopted in order to formulate the rate feedback control part as subcontrollers for RCSMs. Two kinds of output feedback subcontrollers are proposed: a static output feedback control scheme with constant gains which are yielded from the linear–differential-game-based output feedback control; and a dynamic output feedback control scheme which is developed using the Kalman–Yakubovich–Popov Lemma and the linear–differential-game-based state feedback control. Both output feedback control schemes possess robustness to modeling errors, since the stability of the closed-loop systems hinge on the passivity theorem rather than the inertia properties of the retired spacecraft. Numerical simulation results show the effectiveness of the proposed controllers for attitude takeover control of a retired spacecraft fixed with the OCSM and the RCSM. A comparison between the proposed methods and an existing method is carried out to show the benefits of the proposed controllers.

1. Introduction

Thousands of spacecraft have entered into space in the vicinity of the Earth for the past few decades. A remarkable fact is that many spacecraft have retired and become space debris due to malfunction, such as actuator failure [1,2]. The safety of future space missions are jeopardized by these increasingly accumulated space debris. Deorbiting these retired spacecraft is proposed as a solution to accommodate this hazardous situation [3,4]. However, some retired spacecraft only encounter failure on a few components such as actuators, but the rest of their components are still operating well electrically and mechanically. In order to utilize these still-functional high-value space resources, an idea has been put forward in [5] for reusing such retired spacecraft by employing multiple cellularized satellites. Such cellularized satellites cooperate with each other to take over the attitude control of the retired spacecraft. This idea appeared in the DAPRA's Phoenix project in which the antenna of a retired satellite is re-purposed by the cellularized satellites called "Satlet" to create a new space system [5,6]. Another example related to using cellularized satellite is the intelligent Building Blocks for On-orbit-Satellite Servicing (iBOSS) project, in which the standard modular spacecraft are used for on-orbit service and assembly [7,8].

For on-orbit service, attitude takeover control is an important research topic which has been extensively studied in the past few years. The concept of attitude takeover control was initially proposed by Huang et al. [9], where an attitude takeover control scheme for post-capture retired target spacecraft was developed using space robots considering the change of the spacecraft's mass and reaction wheels' configuration. The study of attitude takeover control continued to be explored in [10,11], where the change of thruster configuration was discussed for retired spacecraft's attitude takeover control using a null-space intersection control reallocation method for thrust redistribution. However, none of these studies considered the case of actuator failure. A fault tolerant attitude takeover control scheme was proposed in [12] to tackle a challenge caused by stochastic actuator faults when the retired spacecraft was non-cooperative. These above-mentioned attitude takeover control schemes were all fulfilled by service spacecraft

* Corresponding author.
E-mail addresses: xiaoyu.lang@mail.utoronto.ca (X. Lang), aderuiter@ryerson.ca (A. de Ruiter).

https://doi.org/10.1016/j.actaastro.2021.12.041
Received 5 March 2021; Received in revised form 5 August 2021; Accepted 23 December 2021
Available online 10 January 2022

equipped with robotic manipulators. As an alternative method, multiple cellular space robots were used in a novel attitude takeover control scheme in [13], where a control allocation algorithm was developed specifically for attitude stabilization in a distributed manner. In a similar way, multiple micro-satellites were mounted on a retired spacecraft in [14], and a special attitude takeover control scheme was proposed based on the linear differential game theory for a distributed configuration. Following the method in [14], an event-triggered differential game control scheme was offered in [15] to accommodate disturbances in the process of attitude takeover control. Both [14,15] used linearized spacecraft dynamic models, in which the attitude changes were assumed as infinitesimal angle rotations, to design controllers based on the linear differential game theory. Such linearization, however, is inapplicable for large-angle spacecraft maneuvering. Although in [14] the large-angle spacecraft maneuvering process was split into several small angle rotations, such method made the control system experience several stabilization processes and would hence presumably consume much more control efforts for attitude regulation.

As a common approach utilized in [14,15], linear quadratic differential game theory is a useful strategy to deal with problems in aerospace scenarios which involve several parts (regarded as players in game) to accomplish some particular goals. In [16], two active spacecraft were regarded as two players in a non-zero-sum differential game for rendezvous and motion synchronization. A differential-game-based control scheme was proposed in [17] to stabilize an aeroelastic system, where the gust load was viewed as a player. A satellites proximate interception problem was discussed in [18] where the different thrust configurations were considered as two players in a pursuit-evasion game.

Gain-scheduled control is a powerful method to accommodate nonlinear control problems involving several different system configurations. A gain-scheduled strictly positive real (SPR) control framework was conceived in [19] to control the motion of a flexible robot manipulator which has strong dependence on their dynamic configuration. This control scheme was exploited further in [20] to seek a set of optimal scheduling signals, which can minimize the two-link flexible manipulator's tip tracking errors as well as the control efforts. In [21], a very strictly passive gain-scheduled controller was proposed to overcome actuator saturation while solving the trajectory tracking control for a manipulator with a heavy payload. An input strictly passive gain-scheduled control scheme was studied in [22] using a similar gain-scheduled control framework as shown in [19]. The setup of the gain-scheduled signals and subcontrollers motivates us to design a similar control structure for multiple cellular space modules mounted on the retired spacecraft to execute attitude takeover control. The main contribution of this paper is proposing a new attitude takeover control scheme which combines the differential game theory with the gain-scheduled passivity control to formulate a passivity-based output feedback control scheme for retired spacecraft attitude takeover control. The novelty of this work is implementing the proposed control scheme on the nonlinear spacecraft dynamic plant directly to maintain the stability of the closed-loop system using multiple cellular space modules, while the existing similar control scheme in [14] was established on the basis of a linear model. Additionally, the proposed control scheme has no requirement on the specific knowledge of the inertia property for the retired spacecraft, and hence possesses robustness to dynamic modeling errors. The control torques, which should be provided by all cellular space modules, are calculated by the subcontrollers using the proposed control schemes. There is no need for control allocation.

The rest of this paper is organized as follows. Preliminaries about the linear differential game and passivity theory are reviewed in Section 2, where the problem statement and dynamics formulation are also presented. In Section 3, two control schemes are developed based on the passivity theory and the linear differential game theory. The numerical examples of the proposed control schemes are demonstrated in Section 4. Some conclusion remarks are given in Section 5.

2. Preliminaries

2.1. Linear quadratic differential game control

A general linear time invariant system with n players (inputs) can be described by the following state-space equation:

$$\dot{\boldsymbol{x}} = \boldsymbol{A}\boldsymbol{x} + \sum_{i=1}^{n} \boldsymbol{B}_i \boldsymbol{u}_i \tag{1}$$

where $\boldsymbol{x} \in \mathbb{R}^m$ is the state of this system, $\boldsymbol{u}_i \in \mathbb{R}^{m_i}$ $(i = 1, 2, \dots, n)$ is the system's ith input associated with the player i, and n indicates the total number of players. Each player has its own quadratic cost function defined in an infinite horizon:

$$\mathcal{J}_i(\boldsymbol{x}, \boldsymbol{u}_i, \boldsymbol{u}_{-i}) = \frac{1}{2}\int_0^{\infty} \left[\boldsymbol{x}^\top(t)\boldsymbol{Q}_i\boldsymbol{x}(t) + \sum_{j=1}^{n} \boldsymbol{u}_j^\top(t)\boldsymbol{R}_{ij}\boldsymbol{u}_j(t)\right] \mathrm{d}t \tag{2}$$

where the matrices $\boldsymbol{Q}_i$ and $\boldsymbol{R}_{ij}$ are all positive definite weighting matrices with constant values. An n-tuple optimal control input set $\{\boldsymbol{u}_1^*, \boldsymbol{u}_2^*, \dots, \boldsymbol{u}_n^*\}$ can minimize the cost function $\mathcal{J}_i$ as shown in Eq. (2) if the following conditions (also called Nash equilibrium conditions) are satisfied [23,24].

$$\mathcal{J}_i^* \triangleq \mathcal{J}_i(\boldsymbol{x}, \boldsymbol{u}_1^*, \dots, \boldsymbol{u}_i^*, \dots, \boldsymbol{u}_n^*) \leq \mathcal{J}_i(\boldsymbol{x}, \boldsymbol{u}_1^*, \dots, \boldsymbol{u}_i, \dots, \boldsymbol{u}_n^*) \quad (i = 1, 2, \dots, n) \tag{3}$$

The n-tuple quantities $\{\mathcal{J}_1^*, \mathcal{J}_2^*, \dots, \mathcal{J}_n^*\}$ can represent an n-player game's Nash equilibrium outcome [23,24]. The following optimal state feedback controllers [24] can provide an optimal solution :

$$\boldsymbol{u}_i^* = -\boldsymbol{R}_{ii}^{-1}\boldsymbol{B}_i^\top\boldsymbol{P}_i\boldsymbol{x}(t), \quad (i = 1, 2, \dots, n) \tag{4}$$

which satisfies the Nash equilibrium condition with the dynamic constraint shown in Eq. (1). The matrices $\boldsymbol{P}_i$ $(i = 1, 2, \dots, n)$ are positive definite and can be obtained by solving the following n coupled generalized algebraic Riccati equations [24]:

$$0 = \boldsymbol{P}_i\tilde{\boldsymbol{A}} + \tilde{\boldsymbol{A}}^\top\boldsymbol{P}_i + \boldsymbol{Q}_i - \boldsymbol{P}_i\boldsymbol{B}_i\boldsymbol{R}_{ii}^{-1}\boldsymbol{B}_i^\top\boldsymbol{P}_i + \sum_{j=1, j\neq i}^{n} \boldsymbol{P}_j\boldsymbol{B}_j\boldsymbol{R}_{jj}^{-1}\boldsymbol{R}_{ij}\boldsymbol{R}_{jj}^{-1}\boldsymbol{B}_j^\top\boldsymbol{P}_j \quad (i = 1, 2, \dots, n) \tag{5}$$

where the matrix $\tilde{\boldsymbol{A}}$ is taken as $\tilde{\boldsymbol{A}} = \boldsymbol{A} - \sum_{j=1, j\neq i}^{n} \boldsymbol{B}_j\boldsymbol{R}_{jj}^{-1}\boldsymbol{B}_j^\top\boldsymbol{P}_j$. These n coupled generalized algebraic Riccati equations [Eq. (5)] can be solved by some numerical algorithms, such as the Lyapunov iteration method [25].

2.2. Passivity theory

The input–output stability is an important theory for control system analysis. Some related notions are reviewed herein based on [26]. The 2-norm of a function $\boldsymbol{u}(t)$ is defined as

$$\|\boldsymbol{u}(t)\|_2 = \sqrt{\int_0^{\infty} \boldsymbol{u}^\top(t)\boldsymbol{u}(t)\,\mathrm{d}t} \tag{6}$$

The function $\boldsymbol{u}(t) \in L_2$ if $\|\boldsymbol{u}(t)\|_2 < \infty$. The function $\boldsymbol{u} \in L_{2e}$ if $\|\boldsymbol{u}\|_{2T} = \sqrt{\int_0^T \boldsymbol{u}^\top(t)\boldsymbol{u}(t)\mathrm{d}t} < \infty$, $\forall T > 0$.

Consider a square system whose input is $\boldsymbol{u} \in L_{2e}$ and output is $\boldsymbol{y} \in L_{2e}$. This system can be regarded as an operator $\mathscr{G} : L_{2e} \to L_{2e}$ which can map $\boldsymbol{u}$ into $\boldsymbol{y}$ as $\boldsymbol{y} = \mathscr{G}\boldsymbol{u}$. $\mathscr{G}$ is passive if there exists a positive constant β such that [26]

$$\int_0^T \boldsymbol{y}^\top\boldsymbol{u}\,\mathrm{d}t \geq -\beta, \quad \forall T \in \mathbb{R}^+ \tag{7}$$

When there exists $\gamma > 0$ such that

$$\int_0^T \boldsymbol{y}^\top\boldsymbol{u}\,\mathrm{d}t \geq \gamma\int_0^T \boldsymbol{u}^\top\boldsymbol{u}\,\mathrm{d}t, \quad \forall T \in \mathbb{R}^+ \tag{8}$$

$\mathscr{G}$ is input strictly passive. The celebrated passivity theorem states that the negative interconnection between a passive plant and an input

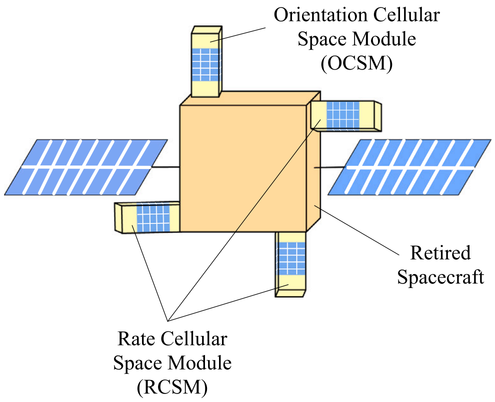

Fig. 1. Combined spacecraft system.

strictly passive controller is endowed with input–output stability [26]. The following lemma is concerned with the passivity notions.

Lemma 1 (*Kalman–Yakubovich–Popov (KYP) lemma [27]*). *Consider a linear time-invariant system:*

$$\begin{aligned}\dot{\boldsymbol{x}}_c &= \boldsymbol{A}_c\boldsymbol{x}_c + \boldsymbol{B}_c\boldsymbol{u}_c\\ \boldsymbol{y}_c &= \boldsymbol{C}_c\boldsymbol{x}_c\end{aligned} \tag{9}$$

where the real matrices $\boldsymbol{A}_c$, $\boldsymbol{B}_c$ and $\boldsymbol{C}_c$ are to form a minimal state-space realization with suitable dimensions, and the matrix $\boldsymbol{A}_c$ is Hurwitz. Its corresponding transfer function is $\boldsymbol{G}(s) = \boldsymbol{C}_c(s\mathbf{1} - \boldsymbol{A}_c)^{-1}\boldsymbol{B}_c$ where $\mathbf{1}$ is an identity matrix. If there exist matrices $\boldsymbol{X} = \boldsymbol{X}^\top > 0$ and $\boldsymbol{Q}_c = \boldsymbol{Q}_c^\top > 0$ such that

$$\boldsymbol{X}\boldsymbol{A}_c + \boldsymbol{A}_c^\top\boldsymbol{X} = -\boldsymbol{Q}_c \tag{10a}$$

$$\boldsymbol{X}\boldsymbol{B}_c = \boldsymbol{C}_c^\top \tag{10b}$$

are satisfied, the system $\boldsymbol{G}(s)$ is a strictly positive real (SPR) system. This SPR system $\boldsymbol{G}(s)$ corresponds to a strictly passive system if an arbitrarily small term δ is added as $\boldsymbol{G}(s) = \boldsymbol{C}_c(s\mathbf{1} - \boldsymbol{A}_c)^{-1}\boldsymbol{B}_c + \delta\mathbf{1}$.

2.3. Problem statement

This paper is concerned with the retired spacecraft which loses its ability to regulate attitude completely. The retired spacecraft is then installed with multiple cellular space modules as an integrated rigid-body combined spacecraft, as depicted in Fig. 1. The attitude control of the retired spacecraft is taken over by these cellular space modules. Each cellular space module is assumed to be equipped with actuators and sensors. In particular, these cellular space modules are categorized as two types, namely orientation cellular space module (OCSM) and rate cellular space module (RCSM). As their names suggested, the OCSM is installed with sensors, such as sun sensors and magnetometers, which can measure two or more unit-length vectors to determine its attitude (orientation). The RCSM is mounted with sensors, such as gyros, which can measure its angular velocity. Practically, it is reasonable to install the sun sensor (or magnetometer) and gyro in separated modules since the sun sensor (or magnetometer) is usually smaller than gyro in terms of size. Both of these two kinds of modules are equipped with mechanical actuators such as reaction wheels which collaboratively provide control torques for the attitude regulation of retired spacecraft. Moreover, the actuators in the OCSM will be responsible for the control torques calculated by the so-called pre-wrap control part which relies on the measurements from sun sensors or magnetometers, and the actuators in the RCSM are responsible for the control torques calculated by the rate feedback part which needs the measurements from gyros. In the subsequent section, the RCSMs will serve as players in the formulation of the game-based controller, while the OCSM is a separated module which is not involved in the game-based controller design. Both the pre-wrap control part and the rate feedback part will be introduced in Section 3.

It is also assumed that the system information of the retired spacecraft, such as inertia properties, can be transmitted among all cellular space modules to proceed the attitude control scheme. The retired spacecraft attitude regulation executed by multiple cellular space modules is formulated as a multi-player non-zero-sum differential game. The objective of this paper is to design a passivity-based control scheme to stabilize the attitude of the combined spacecraft by minimizing the cost functions of the RCSMs under the Nash equilibrium conditions.

2.4. Dynamics formulation

As shown in Fig. 1, the combined spacecraft includes the retired spacecraft and multiple cellular space modules, namely OCSM and RCSM. Several useful coordinate frames are defined for modeling the combined spacecraft. Let $\mathscr{F}_I$ denote the inertial frame. The body-fixed frame of the combined spacecraft is denoted by $\mathscr{F}_B$. Assume that there are n RCSMs and one OCSM installed on the retired spacecraft. The reason of using such number for RCSM and OCSM is set to be compatible with the controller formulation develop in the next section. Denote the body-fixed frame of the jth RCSM $\mathscr{F}_{bj}$ ($j = 1, 2, \dots, n$). The body-fixed frame of the OCSM is denoted by $\mathscr{F}_{bp}$. Assume that $\mathscr{F}_{bj}$ and $\mathscr{F}_{bp}$ are all parallel to the inertia principal axes of the RCSM and OCSM respectively. The transformation from $\mathscr{F}_{bj}$ to $\mathscr{F}_B$ is denoted by a direction cosine matrix $\boldsymbol{\varphi}_j$ ($j = 1, 2, \dots, n$), and the transformation from $\mathscr{F}_{bp}$ to $\mathscr{F}_B$ is represented by another direction cosine matrix $\boldsymbol{\varphi}_p$. It is assumed that the sensors and actuators in OCSM and RCSM are installed parallel to their own body-fixed frames such that the physical quantities measured or provided are all in their own body-fixed frames.

The dynamic model of the combined spacecraft is governed by Euler's rigid-body Equation [28]:

$$\boldsymbol{I}\dot{\boldsymbol{\omega}} + \boldsymbol{\omega}^\times\boldsymbol{I}\boldsymbol{\omega} = \boldsymbol{\tau}_c \tag{11}$$

where $\boldsymbol{I} \in \mathbb{R}^{3\times3}$ denotes the moment of inertia of the combined spacecraft, $\boldsymbol{\omega} \in \mathbb{R}^3$ is the angular velocity vector, and $\boldsymbol{\tau}_c \in \mathbb{R}^3$ is the control input. Note that $\boldsymbol{I}$, $\boldsymbol{\omega}$ and $\boldsymbol{\tau}_c$ are all defined in the frame $\mathscr{F}_B$. The operator $(\cdot)^\times$ is the matrix equivalent form to conduct cross product. For an arbitrary vector $\boldsymbol{a} = \left[a_1, a_2, a_3\right]^\top$, the operation $\boldsymbol{a}^\times$ is given by:

$$\boldsymbol{a}^\times = \begin{bmatrix} 0 & -a_3 & a_2\\ a_3 & 0 & -a_1\\ -a_2 & a_1 & 0\end{bmatrix} \tag{12}$$

Let $(\cdot)^\otimes$ denote the inverse operator of $(\cdot)^\times$ such that $(\boldsymbol{a}^\times)^\otimes = \boldsymbol{a}$.

The angular velocity $\boldsymbol{\omega}$ of the combined spacecraft is measured by the sensors in the RCSMs. Given these RCSMs are fixed on the retired spacecraft as an integrated rigid body, the angular velocities detected by the sensors, such as gyros, installed in the jth ($j = 1, 2, \dots, n$) RCSMs can be expressed as $\boldsymbol{\omega}_j$ defined in the jth RCSM's body frame $\mathscr{F}_{bj}$ such that $\boldsymbol{\omega} = \boldsymbol{\varphi}_j\boldsymbol{\omega}_j$.

As mentioned before, the orientation (attitude) of the combined spacecraft is determined by the sensors in the OCSM. Assume that there are $k = 1, 2, \dots, N$ unit-length vectors which can be measured by the orientation sensors such as sun sensors or magnetometers. Let $\boldsymbol{e}_I^k \in \mathbb{R}^3$ be the kth reference unit-length vector defined in the inertial frame $\mathscr{F}_I$ and they are assumed being linearly independent constant vectors [29]. Let $\boldsymbol{e}^k \in \mathbb{R}^3$ be the kth unit-length vector defined in the OCSM's body frame $\mathscr{F}_{bp}$ such that

$$\boldsymbol{e}^k = \boldsymbol{\varphi}_p^\top\boldsymbol{C}_{BI}\boldsymbol{e}_I^k \tag{13}$$

where $\boldsymbol{C}_{BI}$ is a rotation matrix describing the transformation from $\mathscr{F}_I$ to $\mathscr{F}_B$. Let $\boldsymbol{C}_{DI}$ denote the desired attitude of the combined spacecraft relative to the inertial frame $\mathcal{F}_I$. Hence, the kth desired unit-length vector measurement e_D^k can be written as

$$e_D^k = \varphi_p^\top C_{DI} e_I^k \tag{14}$$

which are also linearly independent vectors [29]. Let $\tilde{e}^k$, defined in the frame $\mathcal{F}_{bp}$, indicate the error between the kth unit-length vector e^k and the desired unit-length vector e_D^k such that [30]

$$\begin{aligned}\tilde{e}^k &= \frac{1}{2}\left(e^k - e_D^k\right)^\top \left(e^k - e_D^k\right) \\ &= 1 - \left(e_D^k\right)^\top e^k\end{aligned} \tag{15}$$

Note that e_D^k is defined in the OCSM's body frame $\mathcal{F}_{bp}$. Using the identity that $a^\top b = \text{trace}\left(ba^\top\right)$ for any column vectors a and b [30] gives

$$\tilde{e}^k = 1 - \text{trace}\left[e^k \left(e_D^k\right)^\top\right] \tag{16}$$

Substitute Eqs. (13) and (14) into Eq. (16) and it arrives at:

$$\begin{aligned}\tilde{e}^k &= 1 - \text{trace}\left[\varphi_p^\top C_{BI} e_I^k \left(e_I^k\right)^\top C_{DI}^\top \varphi_p\right] \\ &= 1 - \text{trace}\left[\varphi_p^\top C_{BI} e_I^k \left(e_I^k\right)^\top C_{BI}^\top \varphi_p \varphi_p^\top C_{BI} C_{DI}^\top \varphi_p\right]\end{aligned} \tag{17}$$

where the properties $\varphi_p \varphi_p^\top = \mathbf{1}$ and $C_{BI}^\top C_{BI} = \mathbf{1}$ are used and these identities will be used in mathematical derivation several times in the sequel. Let $\tilde{C}$ be the error between the current orientation and the desired orientation of the OCSM:

$$\tilde{C} = \varphi_p^\top C_{BI} C_{DI}^\top \varphi_p \tag{18}$$

Then, Eq. (17) can be written as

$$\tilde{e}^k = 1 - \text{trace}\left[\varphi_p^\top C_{BI} e_I^k \left(e_I^k\right)^\top C_{BI}^\top \varphi_p \tilde{C}\right] \tag{19}$$

Assign a weight coefficient η_k ($\eta_k > 0$) to the kth unit-length vector measured by the sensors in the OCSM, the total error $\tilde{e}$ is given by

$$\tilde{e} = \frac{1}{2}\sum_{k=1}^{N} \eta_k \tilde{e}^k = \frac{1}{2}\sum_{k=1}^{N}\left\{\eta_k - \eta_k \text{trace}\left[\varphi_p^\top C_{BI} e_I^k \left(e_I^k\right)^\top C_{BI}^\top \varphi_p \tilde{C}\right]\right\} \tag{20}$$

Let

$$\Xi = \varphi_p^\top C_{BI}\left[\sum_{k=1}^{N} \eta_k e_I^k \left(e_I^k\right)^\top\right] C_{BI}^\top \varphi_p \tag{21}$$

such that the total error $\tilde{e}$ can be reformed as

$$\tilde{e} = \frac{1}{2}\left[\sum_{k=1}^{N} \eta_k - \text{trace}\left(\Xi \tilde{C}\right)\right] \tag{22}$$

The kinematic equation of this combined spacecraft is given by:

$$\dot{C}_{BI} = -\omega^\times C_{BI} \tag{23}$$

For the OCSM, its kinematic equation can be described with the orientation error $\tilde{C}$ defined in Eq. (18) as

$$\dot{\tilde{C}} = \varphi_p^\top \dot{C}_{BI} C_{DI}^\top \varphi_p = -\varphi_p^\top \omega^\times C_{BI} C_{DI}^\top \varphi_p \tag{24}$$

Given $\varphi_p \varphi_p^\top = \mathbf{1}$, Eq. (24) can be written as

$$\dot{\tilde{C}} = -\varphi_p^\top \omega^\times \varphi_p \varphi_p^\top C_{BI} C_{DI}^\top \varphi_p = -\left(\varphi_p^\top \omega\right)^\times \tilde{C} \tag{25}$$

using the identity $b^\times = C_{ba} a^\times C_{ba}^\top$ ($b = C_{ba} a$ for a, $b \in \mathbb{R}^3$, and $C_{ba} \in \mathbb{R}^{3\times3}$ is the rotation matrix between these two vectors). Note that the derivations of Eqs. (13) - (25) are conducted on the basis of Ref. [29].

3. Passivity-based control design using linear quadratic differential game theory

In this section, two passivity-based output feedback control schemes are developed. The first one is a static output feedback control scheme which is derived from the linear–differential-game-based output feedback control theory. This control scheme corresponds to a set of static-gain subcontrollers. The second one is a dynamic output feedback control scheme. This control scheme is formulated by the passivity theory as well as the linear differential game theory. The stability of the closed-loop systems using these two control schemes are guaranteed by the passivity theorem.

3.1. Controller for OCSM

Recall the combined spacecraft's dynamic equation shown in Eq. (11). The total control input τ_c in Eq. (11) is designed as the following form:

$$\tau_c = \varphi_p u_p + u \tag{26}$$

Here, $u_p \in \mathbb{R}^3$ is the pre-wrap control part:

$$u_p = \epsilon r \; (\epsilon > 0) \tag{27}$$

where r is defined as

$$r = \frac{1}{2}\sum_{k=1}^{N} \eta_k (e_D^k)^\times e^k \tag{28}$$

The pre-wrap control part will drive the actuators in the OCSM to generate control torques. Note that u_p is defined in $\mathcal{F}_{bp}$ (body frame of the OCSM) such that it has to be multiplied with the rotation matrix φ_p to constitute the first part of τ_c (defined in the frame $\mathcal{F}_B$).

The second part of τ_c is the rate feedback control part:

$$u = \sum_{j=1}^{n} \varphi_j u_j \tag{29}$$

where $u_j \in \mathbb{R}^3$ (expressed in its body frame $\mathcal{F}_{bj}$) is the control torque vector provided by the jth RCSM.

Based on the total control input defined in Eq. (26), the mapping $\mathcal{G}_E : u \to \omega$ is passive and is proved by the following lemma.

Lemma 2. *$\mathcal{G}_E : u \to \omega$ is passive.*

Proof. Considering the combined spacecraft dynamic Eq. (11) as well as the pre-wrap control in Eq. (27), an energy function is selected as

$$H(t) = \frac{1}{2}\omega^\top I \omega + \frac{1}{2}\epsilon \tilde{e} \tag{30}$$

where $\tilde{e}$ is the total error defined in Eq. (22). Taking time derivative of $H(t)$ gives

$$\dot{H} = \omega^\top I \dot{\omega} - \frac{1}{2}\epsilon\, \text{trace}\left(\dot{\Xi}\tilde{C} + \Xi\dot{\tilde{C}}\right) \tag{31}$$

According Eq. (21), the time derivative of Ξ is given by:

$$\begin{aligned}\dot{\Xi} &= \varphi_p^\top \dot{C}_{BI}\left[\sum_{k=1}^{N} \eta_k e_I^k \left(e_I^k\right)^\top\right] C_{BI}^\top \varphi_p + \varphi_p^\top C_{BI}\left[\sum_{k=1}^{N} \eta_k e_I^k \left(e_I^k\right)^\top\right] \dot{C}_{BI}^\top \varphi_p \\ &= -\varphi_p^\top \omega^\times \varphi_p \varphi_p^\top C_{BI}\left[\sum_{k=1}^{N} \eta_k e_I^k \left(e_I^k\right)^\top\right] C_{BI}^\top \varphi_p \\ &\quad + \varphi_p^\top C_{BI}\left[\sum_{k=1}^{N} \eta_k e_I^k \left(e_I^k\right)^\top\right] C_{BI}^\top \varphi_p \varphi_p^\top \omega \varphi_p \\ &= -\left(\varphi_p^\top \omega\right)^\times \Xi + \Xi\left(\varphi_p^\top \omega\right)^\times\end{aligned} \tag{32}$$

Substituting Eqs. (11), (25), and (32) into Eq. (31) arrives at:

$$\begin{aligned}\dot{H} &= \omega^\top\left(-\omega^\times I\omega + \epsilon\varphi_p r + u\right) \\ &\quad - \frac{1}{2}\epsilon\, \text{trace}\left[-\left(\varphi_p^\top \omega\right)^\times \Xi\tilde{C} + \Xi\left(\varphi_p^\top \omega\right)^\times \tilde{C} - \Xi\left(\varphi_p^\top \omega\right)^\times \tilde{C}\right]\end{aligned} \tag{33}$$

For $\boldsymbol{r}$ defined in Eq. (28), the operation $\boldsymbol{r}^\times$ can be calculated as:

$$
\begin{aligned}
\boldsymbol{r}^\times &= \frac{1}{2}\sum_{k=1}^{N}\eta_k\left[(\boldsymbol{e}_D^k)^\times\boldsymbol{e}^k\right]^\times \\
&= \frac{1}{2}\sum_{k=1}^{N}\eta_k\left[-\boldsymbol{e}_D^k(\boldsymbol{e}^k)^\top+\boldsymbol{e}^k(\boldsymbol{e}_D^k)^\top\right] \\
&= \frac{1}{2}\sum_{k=1}^{N}\eta_k\left[-\boldsymbol{\varphi}_p^\top\boldsymbol{C}_{DI}\boldsymbol{e}_I^k(\boldsymbol{e}_I^k)^\top\boldsymbol{C}_{BI}^\top\boldsymbol{\varphi}_p+\boldsymbol{\varphi}_p^\top\boldsymbol{C}_{BI}\boldsymbol{e}_I^k(\boldsymbol{e}_I^k)^\top\boldsymbol{C}_{DI}^\top\boldsymbol{\varphi}_p\right] \\
&= \frac{1}{2}\sum_{k=1}^{N}\eta_k\left[-\boldsymbol{\varphi}_p^\top\boldsymbol{C}_{DI}\boldsymbol{C}_{BI}^\top\boldsymbol{\varphi}_p\boldsymbol{\varphi}_p^\top\boldsymbol{C}_{BI}\boldsymbol{e}_I^k(\boldsymbol{e}_I^k)^\top\boldsymbol{C}_{BI}^\top\boldsymbol{\varphi}_p\right. \\
&\qquad\left.+\boldsymbol{\varphi}_p^\top\boldsymbol{C}_{BI}\boldsymbol{e}_I^k(\boldsymbol{e}_I^k)^\top\boldsymbol{C}_{BI}^\top\boldsymbol{\varphi}_p\boldsymbol{\varphi}_p^\top\boldsymbol{C}_{BI}\boldsymbol{C}_{DI}^\top\boldsymbol{\varphi}_p\right] \\
&= \frac{1}{2}\left(-\tilde{\boldsymbol{C}}^\top\boldsymbol{\Xi}^\top+\boldsymbol{\Xi}\tilde{\boldsymbol{C}}\right)
\end{aligned}
\tag{34}
$$

This implies that

$$
\boldsymbol{r}=\left[\frac{1}{2}\left(-\tilde{\boldsymbol{C}}^\top\boldsymbol{\Xi}^\top+\boldsymbol{\Xi}\tilde{\boldsymbol{C}}\right)\right]^\otimes \tag{35}
$$

Considering the identity [29]

$$
\mathrm{trace}\left(\boldsymbol{g}^\times\boldsymbol{G}\right)=-\boldsymbol{g}^\top(\boldsymbol{G}-\boldsymbol{G}^\top)^\otimes
$$

as $\boldsymbol{g}\in\mathbb{R}^3$ and $\boldsymbol{G}\in\mathbb{R}^{3\times3}$, Eq. (33) can be rewritten as

$$
\dot{H}=\boldsymbol{\omega}^\top\boldsymbol{u} \tag{36}
$$

Taking integral of both sides over $[0,T]$ gives

$$
\int_0^T\boldsymbol{\omega}^\top\boldsymbol{u}\,\mathrm{d}t=H(T)-H(0)\geq -H(0) \tag{37}
$$

which satisfies Eq. (7). This implies that the mapping $\mathscr{G}_E:\boldsymbol{u}\to\boldsymbol{\omega}$ is passive.

Although the fact that the map $\mathscr{G}_E:\boldsymbol{u}\to\boldsymbol{\omega}$ is passive is well-known and has already shown in [31], the proof of Lemma 2 is still worthwhile to be presented since it involves the coordinate transformation related to the pre-wrap control part shown in Eq. (27). Lemma 2 elaborates that the combined spacecraft dynamic system including the pre-wrap control part, which is a nonlinear plant in the closed-loop system, possesses passivity. Evoking the passivity theorem, an input strictly passive controller is desired here to yield input–output stability. Thus, two output feedback control schemes are developed in the next two subsections, both of which are input strictly passive.

3.2. Static output feedback control for RCSM

The linear quadratic differential game theory is used to formulate the output feedback control. Correspondingly, the nonlinear plant for the combined spacecraft needs to be linearized. According to the infinitesimal angle rotation assumption: $\boldsymbol{C}_{BI}\doteq\mathbf{1}-\boldsymbol{\theta}^\times$ and $\boldsymbol{\omega}\doteq\dot{\boldsymbol{\theta}}$ [28], the Euler's equation and the kinematics equation can be linearized as a linear state space equation by selecting the state $\boldsymbol{x}=\left[\boldsymbol{\theta}^\top,\dot{\boldsymbol{\theta}}^\top\right]^\top$, where $\boldsymbol{\theta}$ and $\dot{\boldsymbol{\theta}}$ are the infinitesimal angle displacement and angular velocities of the combined spacecraft respectively and both are expressed in the frame $\mathscr{F}_B$. Based on [29], the linear form of the pre-wrap control part $\boldsymbol{u}_p$ can be calculated as:

$$
\begin{aligned}
\boldsymbol{u}_p &= \frac{1}{2}\epsilon\sum_{k=1}^{N}\eta_k\left(\boldsymbol{C}_{DI}\boldsymbol{e}_I^k\right)^\times\boldsymbol{e}^k \\
&= \frac{1}{2}\epsilon\sum_{k=1}^{N}\eta_k\boldsymbol{\varphi}_p^\top\boldsymbol{C}_{DI}\boldsymbol{C}_{BI}^\top\boldsymbol{\varphi}_p\boldsymbol{\varphi}_p^\top\boldsymbol{C}_{BI}\left(\boldsymbol{e}_I^k\right)^\times\boldsymbol{C}_{BI}^\top\boldsymbol{\varphi}_p\boldsymbol{\varphi}_p^\top\boldsymbol{C}_{BI}\boldsymbol{C}_{DI}\boldsymbol{\varphi}_p\boldsymbol{e}^k \\
&= \frac{1}{2}\epsilon\sum_{k=1}^{N}\eta_k\tilde{\boldsymbol{C}}^\top\left(\boldsymbol{e}^k\right)^\times\tilde{\boldsymbol{C}}\boldsymbol{e}^k \\
&= \frac{1}{2}\epsilon\sum_{k=1}^{N}\eta_k\left(\tilde{\boldsymbol{C}}^\top\boldsymbol{e}^k\right)^\times\boldsymbol{e}^k
\end{aligned}
\tag{38}
$$

The infinitesimal angle rotation for the OCSM can be approximated as:

$$
\tilde{\boldsymbol{C}}\doteq\boldsymbol{\varphi}_p^\top\left(\mathbf{1}+\boldsymbol{\theta}^\times\right)\boldsymbol{\varphi}_p \tag{39}
$$

Thus,

$$
\begin{aligned}
\boldsymbol{u}_p &\doteq \frac{1}{2}\epsilon\sum_{k=1}^{N}\eta_k\left[\boldsymbol{\varphi}_p^\top\left(\mathbf{1}+\boldsymbol{\theta}^\times\right)\boldsymbol{\varphi}_p\boldsymbol{e}^k\right]^\times\boldsymbol{e}^k \\
&= \frac{1}{2}\epsilon\sum_{k=1}^{N}\eta_k\left[\left(\boldsymbol{\varphi}_p^\top\boldsymbol{\varphi}_p+\boldsymbol{\varphi}_p^\top\boldsymbol{\theta}^\times\boldsymbol{\varphi}_p\right)\boldsymbol{e}^k\right]^\times\boldsymbol{e}^k \\
&= \frac{1}{2}\epsilon\sum_{k=1}^{N}\eta_k\left[\left(\mathbf{1}+(\boldsymbol{\varphi}_p^\top\boldsymbol{\theta})^\times\right)\right]^\times\boldsymbol{e}^k \\
&= \frac{1}{2}\epsilon\sum_{k=1}^{N}\eta_k\left(\boldsymbol{e}^k\right)^\times\left(\boldsymbol{e}^k\right)^\times\boldsymbol{\varphi}_p^\top\boldsymbol{\theta} \\
&= \frac{1}{2}\epsilon\sum_{k=1}^{N}\eta_k\left(\boldsymbol{\varphi}_p^\top\boldsymbol{C}_{BI}\boldsymbol{e}_I^k\right)^\times\left(\boldsymbol{\varphi}_p^\top\boldsymbol{C}_{BI}\boldsymbol{e}_I^k\right)^\times\boldsymbol{\varphi}_p^\top\boldsymbol{\theta}
\end{aligned}
\tag{40}
$$

Hence,

$$
\boldsymbol{\varphi}_p\boldsymbol{u}_p\doteq-\boldsymbol{\Gamma}\boldsymbol{\theta},\quad \boldsymbol{\Gamma}=-\frac{1}{2}\epsilon\boldsymbol{\varphi}_p\sum_{k=1}^{N}\eta_k\left(\boldsymbol{\varphi}_p^\top\boldsymbol{C}_{BI}\boldsymbol{e}_I^k\right)^\times\left(\boldsymbol{\varphi}_p^\top\boldsymbol{C}_{BI}\boldsymbol{e}_I^k\right)^\times\boldsymbol{\varphi}_p^\top \tag{41}
$$

For the sake of simple calculation, $\boldsymbol{\Gamma}$ in Eq. (41) can be regarded as a constant by replacing $\boldsymbol{C}_{BI}$ with $\boldsymbol{C}_{DI}$, which can be understood that the linearization is processed when $\boldsymbol{C}_{BI}$ is close to $\boldsymbol{C}_{DI}$ [29]. Using Eq. (41), the linearized dynamic model for the combined spacecraft attitude control is given by:

$$
\dot{\boldsymbol{x}}=\boldsymbol{A}\boldsymbol{x}+\sum_{j=1}^{n}\boldsymbol{B}_j\boldsymbol{u}_j,\quad \boldsymbol{y}=\boldsymbol{C}\boldsymbol{x} \tag{42}
$$

where

$$
\boldsymbol{A}=\begin{bmatrix}\mathbf{0} & \mathbf{1}\\ -\boldsymbol{I}^{-1}\boldsymbol{\Gamma} & \mathbf{0}\end{bmatrix},\quad \boldsymbol{B}_j=\begin{bmatrix}\mathbf{0}\\ \boldsymbol{I}^{-1}\boldsymbol{\varphi}_j\end{bmatrix},\quad \boldsymbol{C}=\begin{bmatrix}\mathbf{0} & \mathbf{1}\end{bmatrix} \tag{43}
$$

As mentioned before, the jth RCSM has its own rate sensors to measure the angular velocity $\boldsymbol{\omega}_j$ expressed in the frame $\mathscr{F}_{bj}$. Hence, the output of jth RCSM can be written as

$$
\boldsymbol{y}_j=\boldsymbol{\omega}_j=\boldsymbol{\varphi}_j^\top\boldsymbol{\omega}=\boldsymbol{\varphi}_j^\top\boldsymbol{y}=\boldsymbol{C}_j\boldsymbol{x} \tag{44}
$$

where

$$
\boldsymbol{C}_j=\begin{bmatrix}\mathbf{0} & \boldsymbol{\varphi}_j^\top\end{bmatrix} \tag{45}
$$

Define a cost function for the ith RCSM over an infinite-planning horizon as:

$$
\mathcal{J}_i(\boldsymbol{y},\boldsymbol{u}_i,\boldsymbol{u}_{-i})=\frac{1}{2}\int_0^\infty\left[\boldsymbol{y}(t)^\top\boldsymbol{Q}_i\boldsymbol{y}(t)+\sum_{j=1}^{n}\boldsymbol{u}_j(t)^\top\boldsymbol{R}_{ij}\boldsymbol{u}_j(t)\right]\mathrm{d}t \tag{46}
$$

where $\boldsymbol{y}(t)$ is the output of Eq. (42), $\boldsymbol{u}_i$ is the ith control input vector provided by the ith RCSM, and $\boldsymbol{u}_{-i}$ are the control inputs provided by all RCSMs except the ith one. The matrices $\boldsymbol{Q}_i\in\mathbb{R}^{3\times3}$, $\boldsymbol{R}_{ij}\in\mathbb{R}^{3\times3}$ and $\boldsymbol{Q}_{iT}\in\mathbb{R}^{3\times3}$ are all user-defined positive definite weighting matrices with constant values. Considering Eqs. (44)(45), Eq. (46) can be rewritten as

$$
\mathcal{J}_i(\boldsymbol{y}_i,\boldsymbol{u}_i,\boldsymbol{u}_{-i})=\frac{1}{2}\int_0^\infty\left[\boldsymbol{y}_i(t)^\top\boldsymbol{C}_i^\top\boldsymbol{Q}_i\boldsymbol{C}_i\boldsymbol{y}_i(t)+\sum_{j=1}^{n}\boldsymbol{u}_j(t)^\top\boldsymbol{R}_{ij}\boldsymbol{u}_j(t)\right]\mathrm{d}t \tag{47}
$$

The objective of this part is to seek a set of control schemes $\boldsymbol{u}_i^*=\boldsymbol{F}_i\boldsymbol{y}_i(i=1,2\cdots,n)$ to satisfy the following Nash equilibrium condition:

$$
\mathcal{J}_i(\boldsymbol{y}_i,\boldsymbol{u}_1^*,\ldots,\boldsymbol{u}_i^*,\ldots,\boldsymbol{u}_n^*)\leq\mathcal{J}_i(\boldsymbol{y}_i,\boldsymbol{u}_1^*,\ldots,\boldsymbol{u}_i,\ldots,\boldsymbol{u}_n^*),\quad(i=1,2,\ldots,n) \tag{48}
$$

Lemma 3 ([32]). *Consider a multiplayer system expressed as Eqs. (42)(44)(45) with the control input $\boldsymbol{u}_i=\boldsymbol{F}_i\boldsymbol{y}_i(i=1,2\cdots,n)$. There*

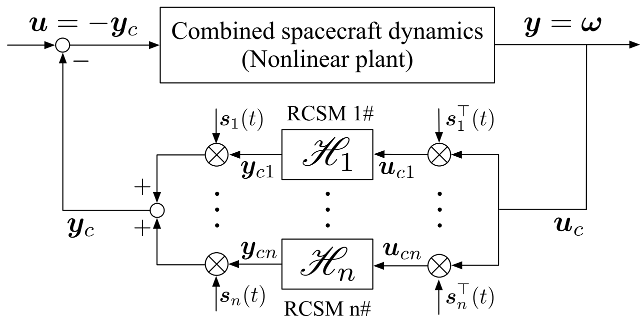

Fig. 2. Output feedback control diagram.

exists the positive definite matrix $\boldsymbol{P}_i$ be the solution of the following equations:

$$0=\boldsymbol{A}^\top\boldsymbol{P}_i+\boldsymbol{P}_i\boldsymbol{A}-\sum_{j=1,j\neq i}^{n}\boldsymbol{P}_i\boldsymbol{B}_j\boldsymbol{R}_{jj}^{-1}\boldsymbol{B}_j^\top\boldsymbol{P}_j-\sum_{j=1,j\neq i}^{n}\boldsymbol{P}_j\boldsymbol{B}_j\boldsymbol{R}_{jj}^{-1}\boldsymbol{B}_j^\top\boldsymbol{P}_i+\boldsymbol{C}_i^\top\boldsymbol{Q}_i\boldsymbol{C}_i$$
$$-\boldsymbol{P}_i\boldsymbol{B}_i\boldsymbol{R}_i{i}^{-1}\boldsymbol{B}_i^\top\boldsymbol{P}_i+\sum_{j=1,j\neq i}^{n}\boldsymbol{P}_j\boldsymbol{B}_j\boldsymbol{R}_{jj}^{-1}\boldsymbol{R}_{ij}\boldsymbol{R}_{jj}^{-1}\boldsymbol{B}_j^\top\boldsymbol{P}_j,\quad(i=1,2,\dots,n) \tag{49}$$

such that

$$\boldsymbol{F}_i=\boldsymbol{R}_{ii}^{-1}\boldsymbol{B}_i^\top\boldsymbol{P}_i\boldsymbol{C}_i^\top\left(\boldsymbol{C}_i\boldsymbol{C}_i^\top\right)^{-1},\quad(i=1,2,\dots,n) \tag{50}$$

are the optimal output feedback gain for $\boldsymbol{u}_i^*=\boldsymbol{F}_i\boldsymbol{y}_i$ satisfying the Nash equilibrium condition shown in Eq. (48).

The positive definite solution $\boldsymbol{P}_i$ of Eq. (49) can be calculated using Lyapunov iteration [25] since $\boldsymbol{C}_i^\top\boldsymbol{Q}_i\boldsymbol{C}_i$ is positive semi-definite and $\boldsymbol{R}_{ii},\boldsymbol{R}_{ij}$ are positive definite. Note that Lemma 3 is developed based on the linear system shown in Eq. (42) which is inapplicable to be implemented on the nonlinear systems. We adopt a gain-scheduled control framework from [19] to design the subcontrollers for RCSMs such that the controller can stabilize the attitude of the nonlinear plant of the combined spacecraft shown in Eq. (11).

Theorem 1. *Consider a control scheme shown in Fig. 2.*

The controller $\mathscr{H}_i$ for the ith RCSM is designed as

$$\boldsymbol{y}_{ci}=\boldsymbol{R}_{ii}^{-1}\boldsymbol{B}_i^\top\boldsymbol{P}_i\boldsymbol{C}_i^\top\left(\boldsymbol{C}_i\boldsymbol{C}_i^\top\right)^{-1}\boldsymbol{u}_{ci} \tag{51}$$

where $\boldsymbol{y}_{ci}$ is the output of the controller $\mathscr{H}_i$, $\boldsymbol{u}_{ci}=\boldsymbol{y}_i=\boldsymbol{s}_i\boldsymbol{y}$ is the input of the controller $\mathscr{H}_i$, and the positive definite matrix $\boldsymbol{P}_i(t)\in\mathbb{R}^{3\times3}$ is obtained by solving Eq. (49). The scheduling signal $\boldsymbol{s}_i$ is selected as $\boldsymbol{s}_i=\boldsymbol{\varphi}_i$. The parameter matrix $\boldsymbol{R}_{ii}$ is set as the form $\boldsymbol{R}_{ii}=r_{ii}\boldsymbol{\varphi}_i^\top\boldsymbol{I}\boldsymbol{\varphi}_i$ where r_{ii} is a positive constant. The controller including $\mathscr{H}_i$ and the scheduling signal $\boldsymbol{s}_i$ can guarantee the input–output stability of the closed-loop system.

Proof. Define $\boldsymbol{W}_i=\boldsymbol{R}_{ii}^{-1}\boldsymbol{B}_i^\top\boldsymbol{P}_i\boldsymbol{C}_i^\top\left(\boldsymbol{C}_i\boldsymbol{C}_i^\top\right)^{-1}$ such that the ith control scheme in Eq. (51) can be simply written as

$$\boldsymbol{y}_{ci}=\boldsymbol{W}_i\boldsymbol{u}_{ci} \tag{52}$$

Given the matrices $\boldsymbol{R}_{ii}=r_{ii}\boldsymbol{\varphi}_i^\top\boldsymbol{I}\boldsymbol{\varphi}_i$ and $\boldsymbol{P}_i$ are positive definite, substituting the forms of $\boldsymbol{B}_i$ and $\boldsymbol{C}_i$ from Eqs. (43)(45) into $\boldsymbol{W}_i$ deduces that $\boldsymbol{W}_i$ is positive definite (The proof of this claim is presented in Appendix). Let λ_i denote the minimum eigenvalue of the matrix $\boldsymbol{W}_i$ and we have $\lambda_i>0$. For the controller $\mathscr{H}_i$, integrating the product of its input $\boldsymbol{u}_{ci}$ and output $\boldsymbol{y}_{ci}$ gives

$$\int_0^T\boldsymbol{y}_{ci}^\top\boldsymbol{u}_{ci}\,\mathrm{d}t=\int_0^T\boldsymbol{u}_{ci}^\top\boldsymbol{W}_i\boldsymbol{u}_{ci}\,\mathrm{d}t\geq\lambda_i\int_0^T\boldsymbol{u}_{ci}^\top\boldsymbol{u}_{ci}\,\mathrm{d}t \tag{53}$$

This implies that $\mathscr{H}_i$ is input strictly passive. Then, consider the integral:

$$\begin{aligned}\int_0^T\boldsymbol{y}_c^\top\boldsymbol{u}_c\,\mathrm{d}t&=\int_0^T\boldsymbol{u}_c^\top\sum_{i=1}^{n}\boldsymbol{s}_i\boldsymbol{y}_{ci}\,\mathrm{d}t\\&=\sum_{i=1}^{n}\int_0^T\boldsymbol{y}_{ci}^\top\boldsymbol{u}_{ci}\,\mathrm{d}t\\&\geq\sum_{i=1}^{n}\lambda_i\|\boldsymbol{u}_{ci}\|_{2T}^2\\&=\sum_{i=1}^{n}\lambda_i\int_0^T\boldsymbol{u}_c^\top\boldsymbol{s}_i\boldsymbol{s}_i^\top\boldsymbol{u}_c\,\mathrm{d}t\end{aligned} \tag{54}$$

Since $\boldsymbol{s}_i\boldsymbol{s}_i^\top=\boldsymbol{\varphi}_i\boldsymbol{\varphi}_i^\top=\boldsymbol{1}$, one has that:

$$\int_0^T\boldsymbol{y}_c^\top\boldsymbol{u}_c\,\mathrm{d}t\geq\bar{\lambda}\|\boldsymbol{u}_c\|_{2T}^2 \tag{55}$$

where $\bar{\lambda}=\sum_{i=1}^{n}\lambda_i>0$. This implies that the controller $\mathscr{H}$ including the subcontrollers $\mathscr{H}_i$ $(i=1,2,\dots,n)$ as well as the scheduling signals $\boldsymbol{s}_i$ $(i=1,2,\dots,n)$ is strictly passive. As it is negatively interconnected with the passive nonlinear plant as depicted in Fig. 2, the closed-loop system is input–output stable guaranteed by the passivity theorem.

Remark 1. Linearized dynamic model shown in Eq. (42) is only used to facilitate the controller design. The original nonlinear plant of the combined spacecraft [Eq. (11)] will be negatively interconnected with the proposed controller to fulfill the attitude takeover control.

Remark 2. The key parameters in the control scheme are the matrices $\boldsymbol{P}_i\,(i=1,2,\dots,n)$ which are the solutions of Eq. (49). The matrices $\boldsymbol{P}_i$ seemingly allocate the control proportion to each RCSM, but this proposed scheme has no need for control allocation.

Remark 3. In this work, the number of RCSM and OCSM are set as n and one respectively. Such setup is designed to be compatible with the controller formulation. In particular, the proposed game-based controller is implemented only among RCSMs. The proposed output feedback control should employ n players (RCSMs) to proceed the calculation based on the game theory. Hence, the number of RCSM is set as n. The pre-wrap proportional control part does not serve as players in the game theory. It is an independent part in the proposed controller, and thus one OCSM is used to provide the torques calculate by this part. The pre-wrap proportional control part could also be distributed if multiple OCSMs are used. It simply becomes a control allocation problem among the OCSMs. The implemented control law is the same as if there is only one OCSM.

Remark 4. Note that the ith RCSM can calculate its own control input $\boldsymbol{u}_i=\boldsymbol{F}_i\boldsymbol{y}_i$ by optimizing the individual performance index function shown in Eq. (46) independently. All RCSMs and OCSM collaborate in a coordinated way to achieve the attitude regulation of the retired spacecraft. The proposed schemes are executed by all cellular space modules to solve the attitude takeover control problem in a network. All cellular space modules can communicate and interact with each other in this network to obtain the full state information of the entire dynamic system. This network has no central fusion but consists of multiple cellular space modules which can implement their own subcontrollers individually.

3.3. Dynamic output feedback control for RCSM

Analogously to the static output feedback control displayed in Section 3.2, the total control input $\boldsymbol{\tau}_c$ for the combined spacecraft in this part is likewise set as

$$\boldsymbol{\tau}_c = \boldsymbol{u}_p + \bar{\boldsymbol{u}} \tag{56}$$

where the pre-wrap control part $\boldsymbol{u}_p$ is identical to Eq. (27) and is also provided by the actuators installed in the OCSM. $\bar{\boldsymbol{u}}$ is the dynamic rate feedback control part:

$$\bar{\boldsymbol{u}} = \sum_{j=1}^{n} \boldsymbol{\varphi}_j \boldsymbol{u}_j \tag{57}$$

The dynamic rate feedback control part is negatively interconnected with the combined spacecraft as shown in Fig. 2 but $\boldsymbol{u}$ is replaced by $\bar{\boldsymbol{u}}$. The specific form of this dynamic controller is given in the following theorem.

Theorem 2. *Consider a control scheme as shown in Fig. 2. The sub-control scheme $\mathscr{H}_i$ for the ith RCSM is defined as*

$$\dot{\boldsymbol{x}}_{ci} = \boldsymbol{A}_{ci}\boldsymbol{x}_{ci} + \boldsymbol{B}_{ci}\boldsymbol{u}_{ci}, \boldsymbol{y}_{ci} = \boldsymbol{C}_{ci}\boldsymbol{x}_{ci} \tag{58}$$

where $\boldsymbol{x}_{ci}$ is the state of the dynamic output feedback controller for the ith RCSM, and the matrices $\boldsymbol{A}_{ci}$, $\boldsymbol{B}_{ci}$ and $\boldsymbol{C}_{ci}$ satisfy the following conditions:

$$\boldsymbol{A}_{ci}^\top \boldsymbol{X}_{ci} + \boldsymbol{X}_{ci}\boldsymbol{A}_{ci} = -\boldsymbol{Q}_{ci} \tag{59a}$$

$$\boldsymbol{X}_{ci}\boldsymbol{B}_{ci} = \boldsymbol{C}_{ci}^\top \tag{59b}$$

where $\boldsymbol{X}_{ci} = \boldsymbol{X}_{ci}^\top > 0$ and $\boldsymbol{Q}_{ci} = \boldsymbol{Q}_{ci}^\top > 0$. The scheduling signal s_i is set as $s_i = \boldsymbol{\varphi}_i$. The controller $\tilde{\mathscr{H}}$ including the dynamic controllers $\mathscr{H}_i$ shown in Eq. (58) as well as the scheduling signals s_i can guarantee the asymptotic stability of the attitude of the retired spacecraft equipped with multiple cellular space modules.

Proof. Consider the following Lyapunov candidate:

$$V_{\text{Lyap}} = \frac{1}{2}\boldsymbol{\omega}^\top \boldsymbol{I}\boldsymbol{\omega} + \frac{1}{2}\epsilon\tilde{e} + \frac{1}{2}\sum_{i=1}^{n} \boldsymbol{x}_{ci}^\top \boldsymbol{X}_{ci}\boldsymbol{x}_{ci} \tag{60}$$

Considering the controller shown in Fig. 2 and Eqs. (11)(22)(57)(58)(59), taking time derivative of V_{Lyap} has

$$\begin{aligned}
\dot{V}_{\text{Lyap}} &= \boldsymbol{\omega}^\top \boldsymbol{I}\dot{\boldsymbol{\omega}} - \frac{1}{2}\epsilon\,\text{trace}\left(\dot{\boldsymbol{\Xi}}\tilde{\boldsymbol{C}} + \boldsymbol{\Xi}\dot{\tilde{\boldsymbol{C}}}\right) + \sum_{i=1}^{n} \boldsymbol{x}_{ci}^\top \boldsymbol{X}_{ci}(\boldsymbol{A}_{ci}\boldsymbol{x}_{ci} + \boldsymbol{B}_{ci}\boldsymbol{s}_i^\top\boldsymbol{\omega}) \\
&= \boldsymbol{\omega}^\top\bar{\boldsymbol{u}} + \sum_{i=1}^{n}\left[\frac{1}{2}\boldsymbol{x}_{ci}^\top\left(\boldsymbol{X}_{ci}\boldsymbol{A}_{ci} + \boldsymbol{A}_{ci}^\top\boldsymbol{X}_{ci}\right)\boldsymbol{x}_{ci} + \boldsymbol{x}_{ci}^\top\boldsymbol{X}_{ci}\boldsymbol{B}_{ci}\boldsymbol{s}_i^\top\boldsymbol{\omega}\right] \\
&= \boldsymbol{\omega}^\top\bar{\boldsymbol{u}} + \sum_{i=1}^{n}\left[-\frac{1}{2}\boldsymbol{x}_{ci}^\top\boldsymbol{Q}_{ci}\boldsymbol{x}_{ci} + \boldsymbol{x}_{ci}^\top\boldsymbol{C}_{ci}^\top\boldsymbol{s}_i^\top\boldsymbol{\omega}\right] \\
&= -\frac{1}{2}\sum_{i=1}^{n}\boldsymbol{x}_{ci}^\top\boldsymbol{Q}_{ci}\boldsymbol{x}_{ci} \le 0
\end{aligned} \tag{61}$$

Given $\boldsymbol{Q}_{ci} = \boldsymbol{Q}_{ci}^\top > 0$, $\dot{V}_{\text{Lyap}} = 0$ holds as $\boldsymbol{x}_{ci} = \boldsymbol{0}$. This implies that $\dot{\boldsymbol{x}}_{ci} = \boldsymbol{0}$ and $\boldsymbol{y}_{ci} = \boldsymbol{0}$, which means $\boldsymbol{u} = -\sum_{i=1}^{n} s_i\boldsymbol{y}_{ci} = \boldsymbol{0}$. Owing that all $\boldsymbol{B}_{ci}(i = 1, 2, \dots, n)$ have full column rank, one arrives at $\boldsymbol{\omega} = \boldsymbol{0}$. It follows that $\dot{\boldsymbol{\omega}} = \boldsymbol{0}$. Hence, according to LaSalle's theorem and Eqs. (18)(23), $(\tilde{\boldsymbol{C}}, \boldsymbol{\omega}, \boldsymbol{x}_{ci}) \to (\boldsymbol{1}, \boldsymbol{0}, \boldsymbol{0})$ as $t \to \infty$.

Algorithm 1 Steps to formulate the dynamic output feedback control given in Eq. (58)

1: Recall the linearized spacecraft attitude dynamic model as shown in Eqs. (42)(43).

2: Consider a cost function in an infinite time horizon for each RCSM as

$$\mathcal{K}_i(\boldsymbol{x}, \boldsymbol{u}_i, \boldsymbol{u}_{-i}) = \frac{1}{2}\int_0^\infty \left(\boldsymbol{x}(t)^\top\boldsymbol{Q}_{d_i}\boldsymbol{x}(t) + \sum_{j=1}^{n}\boldsymbol{u}_j(t)^\top\boldsymbol{R}_{d_{ij}}\boldsymbol{u}_j(t)\right)\mathrm{d}t.$$

where $\boldsymbol{Q}_{d_i} = \boldsymbol{Q}_{d_i}^\top \in \mathbb{R}^{6\times6}$ and $\boldsymbol{R}_{d_{ij}} = \boldsymbol{R}_{d_{ij}}^\top \in \mathbb{R}^{3\times3}$ are user-defined positive definite matrices.

3: Using the Lyapunov iteration method [25], calculate the positive definite matrix $\boldsymbol{U}_{ci} \in \mathbb{R}^{6\times6}$ by solving the following coupled generalized algebraic Riccati equations:

$$\begin{aligned}
0 = &\left(\boldsymbol{A} - \sum_{j=1,j\neq i}^{n}\boldsymbol{B}_j\boldsymbol{R}_{d_{jj}}^{-1}\boldsymbol{B}_j^\top\boldsymbol{U}_{cj}\right)^\top\boldsymbol{U}_{ci} + \boldsymbol{U}_{ci}\left(\boldsymbol{A} - \sum_{j=1,j\neq i}^{n}\boldsymbol{B}_j\boldsymbol{R}_{d_{jj}}^{-1}\boldsymbol{B}_j^\top\boldsymbol{U}_{cj}\right) \\
&- \boldsymbol{U}_{ci}\boldsymbol{B}_i\boldsymbol{R}_{d_{ii}}^\top\boldsymbol{B}_i^\top\boldsymbol{U}_{ci} + \sum_{j=1,j\neq i}^{n}\boldsymbol{U}_{cj}\boldsymbol{B}_j\boldsymbol{R}_{d_{jj}}^{-1}\boldsymbol{R}_{d_{ij}}\boldsymbol{R}_{d_{jj}}^{-1}\boldsymbol{B}_j^\top\boldsymbol{U}_{cj}, (i = 1, 2, \cdots, n)
\end{aligned}$$

4: Solve this optimal control problem using linear differential game theory under Nash equilibrium condition to get the state feedback gain $\boldsymbol{C}_{ci} = \boldsymbol{R}_{d_{ii}}^{-1}\boldsymbol{B}_i^\top\boldsymbol{U}_{ci}$, $(i = 1, 2, \cdots, n)$.

5: Formulate the matrix $\boldsymbol{A}_{ci} = \boldsymbol{A} - \sum_{j=1,j\neq i}^{n}\boldsymbol{B}_j\boldsymbol{R}_{d_{jj}}^\top\boldsymbol{B}_j^\top\boldsymbol{U}_{cj}$.

6: Pick the matrix $\boldsymbol{Q}_{ci}$ as

$$\boldsymbol{Q}_{ci} = \boldsymbol{Q}_{d_i} + \boldsymbol{U}_{ci}\boldsymbol{B}_i\boldsymbol{R}_{d_{ii}}^\top\boldsymbol{B}_i^\top\boldsymbol{U}_{ci} + \sum_{j=1,j\neq i}^{n}\boldsymbol{U}_{cj}\boldsymbol{B}_j\boldsymbol{R}_{d_{jj}}^{-1}\boldsymbol{R}_{d_{ij}}\boldsymbol{R}_{d_{jj}}^{-1}\boldsymbol{B}_j^\top\boldsymbol{U}_{cj}$$

7: Solve Eq. (59a) to have the positive definite matrix $\boldsymbol{X}_{ci}$

8: Determine the matrix $\boldsymbol{B}_{ci}$ from Eq. (59b) as $\boldsymbol{B}_{ci} = \boldsymbol{X}_{ci}^{-1}\boldsymbol{C}_{ci}^\top$

Remark 5. Compared with the proof of Theorem 2, the proof of Theorem 1 is presented based on the theory of input–output stability such that the LaSalle's theorem is not used.

For the ith control scheme given in Eq. (58), Theorem 2 only provides the properties of $\boldsymbol{A}_{ci}$, $\boldsymbol{B}_{ci}$ and $\boldsymbol{C}_{ci}$. The specific forms of these matrices are not presented yet. There are various methods to formulate this dynamic output feedback controller. In this paper, the linear quadratic game theory is employed to formulate the form of $\boldsymbol{A}_{ci}$, $\boldsymbol{B}_{ci}$ and $\boldsymbol{C}_{ci}$, which is another contribution of this paper. The formulation details are given in Algorithm 1.

Remark 6. The connection of these two kinds of sub-controllers is that the common control structure (as shown in Fig. 2) is used by these two schemes to formulate their own feedback control. The difference between them is that the forms of these two kinds are established through two distinct ways. The static output feedback control scheme is obtained from differential game theory to obtain a static gain. The dynamic one is established from a dynamic controller [Eq. (58)] whose parameters are formulated by the KYP lemma.

4. Numerical examples

In this section, the proposed static output feedback controller in Eq. (51) and the dynamic feedback controller in Eq. (58) will be sepetately applied on the nonlinear spacecraft attitude dynamics shown in Eq. (11). The physical parameters of the combined spacecraft are given as follows. The moment of inertia matrix $\boldsymbol{I}$ for the combined spacecraft is set as

$$\boldsymbol{I} = \begin{bmatrix} 1051.53 & -37.41 & 48.69 \\ -37.41 & 939.21 & -25.83 \\ 48.69 & -25.83 & 679.26 \end{bmatrix}\text{kg}\cdot\text{m}^2$$

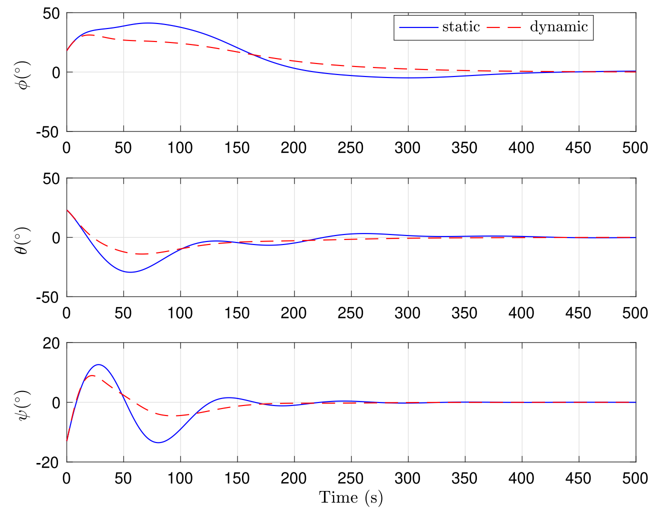

Fig. 3. Euler angles verse time using static and dynamic output feedback controllers.

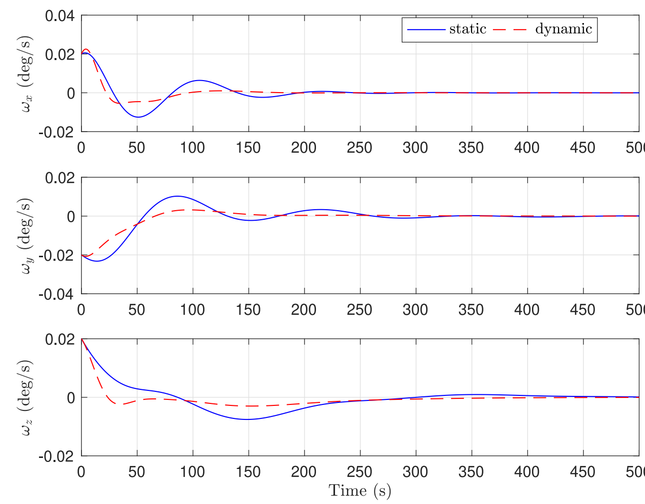

Fig. 4. Angular velocities $\boldsymbol{\omega}$ verse time using static and dynamic output feedback controllers.

which is defined in the frame $\mathscr{F}_B$. In this simulation, three RCSMs and one OCSM are mounted on the retired spacecraft, as depicted in Fig. 1. The direction cosine matrices for the RCSMs and OCSM are set as $\boldsymbol{\varphi}_1 = \boldsymbol{\varphi}_{e1}\boldsymbol{C}_z(41.89°)\boldsymbol{C}_y(-52.15°)\boldsymbol{C}_x(-18.96°)$, $\boldsymbol{\varphi}_2 = \boldsymbol{\varphi}_{e2}\boldsymbol{C}_z(0°)\boldsymbol{C}_y(-28°)\boldsymbol{C}_x(-90.1°)$, $\boldsymbol{\varphi}_3 = \boldsymbol{\varphi}_{e3}\boldsymbol{C}_z(-37°)\boldsymbol{C}_y(0°)\boldsymbol{C}_x(180.1°)$ and $\boldsymbol{\varphi}_p = \boldsymbol{\varphi}_{ep}\boldsymbol{C}_z(9.89°)\boldsymbol{C}_y(2.09°)\boldsymbol{C}_x(8.92°)$ where $\boldsymbol{C}_{(*)}$ is the rotation matrix with respect to $(*)$ axis. The error rotation matrices are set as $\boldsymbol{\varphi}_{e1} = \boldsymbol{C}_z(0.1° \times \sin(0.05t))\boldsymbol{C}_y(0.2° \times \cos(0.05t))\boldsymbol{C}_x(0.15° \times \sin(0.05t))$, $\boldsymbol{\varphi}_{e2} = \boldsymbol{C}_z(0.2° \times \cos(0.06t))\boldsymbol{C}_y(0.15° \times \sin(0.06t))\boldsymbol{C}_x(0.1° \times \cos(0.06t))$, $\boldsymbol{\varphi}_{e3} = \boldsymbol{C}_z(0.15° \times \sin(0.07t))\boldsymbol{C}_y(0.1° \times \cos(0.07t))\boldsymbol{C}_x(0.2° \times \sin(0.07t))$ and $\boldsymbol{\varphi}_{ep} = \boldsymbol{C}_z(0.1° \times \cos(0.08t))\boldsymbol{C}_y(0.15° \times \sin(0.08t))\boldsymbol{C}_x(0.2° \times \cos(0.08t))$. They are considered in simulation since the direction cosine matrices for the RCSMs and OCSM cannot be known exactly. The initial attitude of the combined spacecraft is given in the form of Euler angles $[18°, 23°, -13°]^{\top}$ with the rotation order zyx to yield the rotation matrix $\boldsymbol{C}_{BI}$. The initial angular velocities of the combined spacecraft are set as $\boldsymbol{\omega}_0 = [0.02, -0.02, 0.02]^{\top}$ rad/s which is expressed in the frame $\mathscr{F}_B$. For the OCSM, the reference unit-length vector measurements are set as $\boldsymbol{e}_I^1 = [0, 0, 1]^{\top}$ and $\boldsymbol{e}_I^2 = [0, 0.6614, 0.75]^{\top}$ expressed in the frame $\mathscr{F}_I$. The weight coefficients used in Eq. (20) are set as $\eta_1 = \eta_2 = 1$. The desired attitude of the combined spacecraft is set as $\boldsymbol{C}_{DI} = \boldsymbol{1}_{3\times3}$. The disturbance torque $\boldsymbol{\tau}_d$ is considered in the simulation, and it is given as: $\boldsymbol{\tau}_d = [0.025 \times \sin(0.2t), 0.028 \times \sin(0.2t), 0.023 \times \sin(0.25t)]^{\top}$ N · m. The above parameters are the commonly used by the static output feedback control and the dynamic output feedback control in the simulation.

4.1. Simulation descriptions

The controller formulated in Sections 3.2 and 3.3 are implemented to drive the actuators in RCSM for attitude takeover control. The parameters in Theorem 1 are selected as follows. The constant ϵ in the pre-wrap control part in Eq. (27) is set as $\epsilon = 2.55$ N · m. The weighting matrices used in the cost function, Eq. (47), are set as: $\boldsymbol{Q}_1 = \boldsymbol{Q}_2 = \boldsymbol{Q}_3 = 5.9 \times \boldsymbol{1}_{3\times3}$, $r_{11} = r_{22} = r_{33} = 0.043$, $\boldsymbol{R}_{12} = \boldsymbol{R}_{13} = \boldsymbol{R}_{21} = \boldsymbol{R}_{23} = \boldsymbol{R}_{31} = \boldsymbol{R}_{32} = 0.043 \times \boldsymbol{1}_{3\times3}$. The parameters used in Algorithm 1 are given as follows. The weight matrices in the step 2 are selected as: $\boldsymbol{Q}_{d_1} = \boldsymbol{Q}_{d_2} = \boldsymbol{Q}_{d_3} = 6.9 \times \boldsymbol{1}_{6\times6}$, $\boldsymbol{R}_{d_{11}} = \boldsymbol{R}_{d_{22}} = \boldsymbol{R}_{d_{33}} = 0.038 \times \boldsymbol{1}_{3\times3}$, $\boldsymbol{R}_{d_{12}} = \boldsymbol{R}_{d_{13}} = \boldsymbol{R}_{d_{21}} = \boldsymbol{R}_{d_{23}} = \boldsymbol{R}_{d_{31}} = \boldsymbol{R}_{d_{32}} = 0.038 \times \boldsymbol{1}_{3\times3}$. The parameter in the pre-wrap term is also set as $\epsilon = 2.55$ N · m.

Under the static output feedback controller formulated in Theorem 1 and the dynamic output feedback controller formulated in Algorithm 1, the time responses of the Euler angles and the angular velocities $\boldsymbol{\omega}$ are shown in Fig. 3 and Fig. 4 respectively. Both figures show that the attitude of the combined spacecraft can be stabilized by

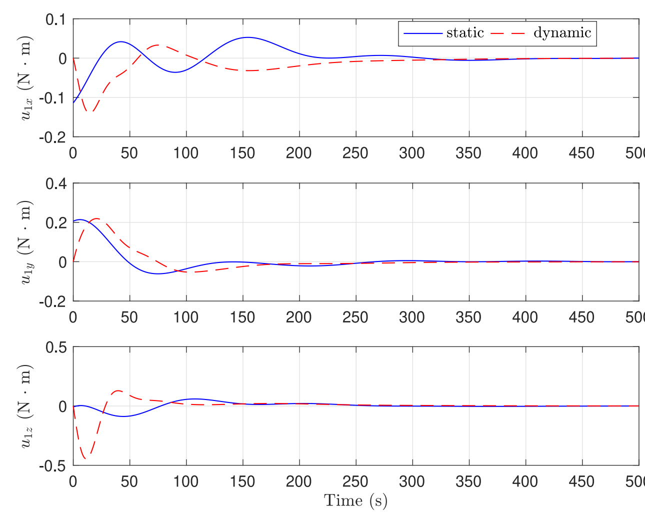

Fig. 5. Control torque $\boldsymbol{u}_1$ verse time using static and dynamic output feedback controllers.

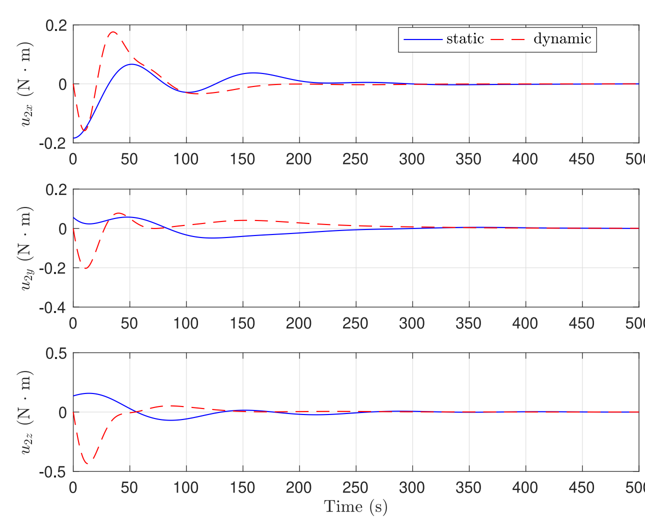

Fig. 6. Control torque $\boldsymbol{u}_2$ verse time using static and dynamic output feedback controllers.

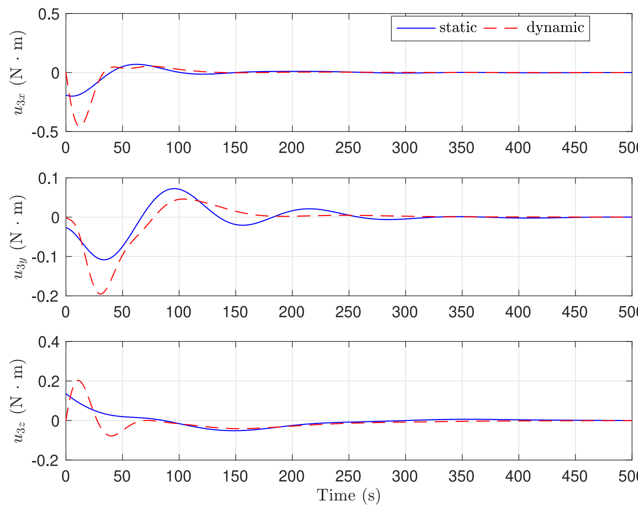

Fig. 7. Control torque $\boldsymbol{u}_3$ verse time using static and dynamic output feedback controllers.

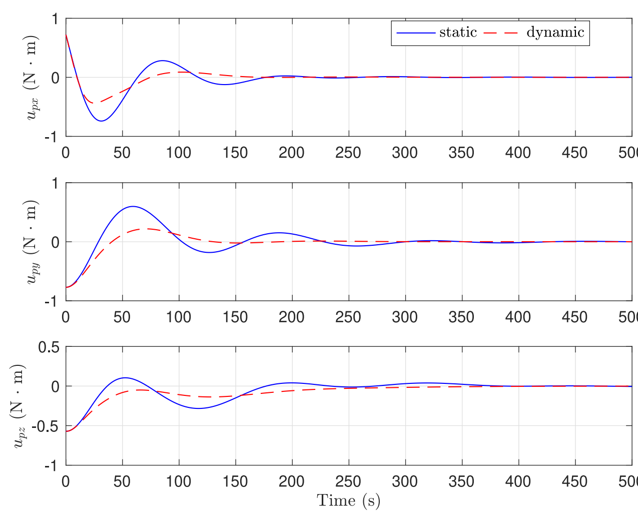

Fig. 8. Control torque $\boldsymbol{u}_p$ verse time using static and dynamic output feedback controllers.

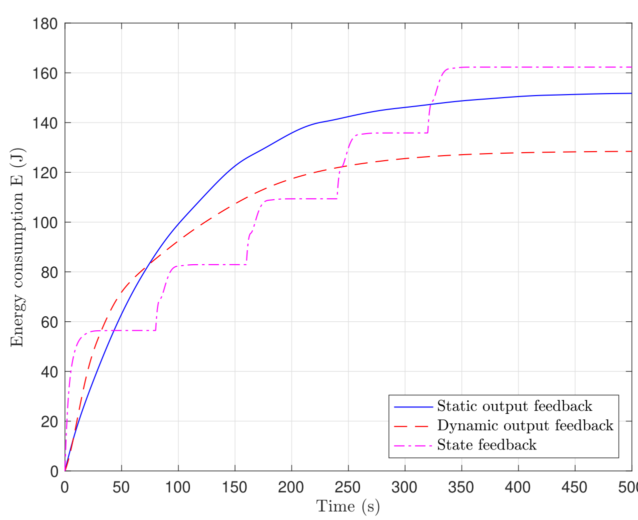

Fig. 9. Energy consumption indices E using the static output feedback, dynamic output feedback, and the state feedback control proposed in [14].

the OCSM and RCSMs within 400 s. From Figs. 3 and 4, it can be noticed that the dynamic output feedback controller has better performance in terms of the Euler angles and angular velocities compared with the static output feedback controller. The control torques provided by three RCSMs and one OCSM are illustrated in Figs. 5–8. Note that the control torques $\boldsymbol{u}_1$, $\boldsymbol{u}_2$, $\boldsymbol{u}_3$ and $\boldsymbol{u}_p$ are all expressed in their own body frames, which represent the control commands driving their own actuators to produce torques for attitude regulation of the combined spacecraft. All above simulation results show the effectiveness of the proposed two game-based output feedback control schemes. For the RCSMs' control torques, the magnitudes of $\boldsymbol{u}_1$, $\boldsymbol{u}_2$, and $\boldsymbol{u}_3$ using the static controller are smaller than these magnitudes using the dynamic controller. As shown in Fig. 8, the static controller has larger magnitudes of $\boldsymbol{u}_p$ compared with the dynamic controllers. This is mainly caused by the different properties of these two controllers. Specifically, the dynamic output feedback control scheme is based on the controller given in Eq. (58). Its controller state $\boldsymbol{x}_{ci}$ can vary adaptively along with the change of the angular velocity during the transient process, while the static control scheme just depends on the angular velocity with a static gain yielded from the game theory. It is a highly possible reason why better performance can be attained by the dynamic control scheme compared with the static one.

The state feedback control based on the linear differential game theory proposed in [14] for large angle attitude stabilization is regenerated for making a comparison with the two output feedback control schemes in terms of the control effort. An energy consumption index E is defined as:

$$E(t) = \frac{1}{t}\int_0^t \sum_{i=1}^{n} \|\boldsymbol{u}_i(\tau)\|_2 \mathrm{d}\tau \tag{62}$$

where $\boldsymbol{u}_i$ is the control torque for cellular space modules (including OCSM and RCSM) in this paper or for each players in [14]. The inertia parameters, the initial angular velocities and the initial Euler angles are retained as the values used in the previous part of this paper. The parameters for the controller developed in [14] is set as $\boldsymbol{Q}_1 = \boldsymbol{Q}_2 = \boldsymbol{Q}_3 = 0.5 \times \mathbf{1}_{3\times3}$, $\boldsymbol{R}_{11} = \boldsymbol{R}_{22} = \boldsymbol{R}_{33} = 0.001 \times \mathbf{1}_{3\times3}$, $\boldsymbol{R}_{12} = \boldsymbol{R}_{13} = \boldsymbol{R}_{21} = \boldsymbol{R}_{23} = \boldsymbol{R}_{31} = \boldsymbol{R}_{32} = 0.0005 \times \mathbf{1}_{3\times3}$ where $\mathbf{1}$ is the identity matrix. The transient time in the control process under the state feedback control [14] is around 400 s, but the evolution of angular velocities has to experience several transient processes (see Fig. 11 in [14]). The comparison of the energy consumption indices under the static output feedback, dynamic output feedback, and the state feedback control in [14] is depicted in Fig. 9. It can be noticed that the static control scheme has the lowest energy consumption. Both proposed control schemes have lower numbers compared with the state feedback control. The differences between the control schemes proposed in this paper and the state feedback control developed in [14] are twofold. The first one is the control schemes proposed in this paper are applicable to the nonlinear plant of the combined spacecraft, while the state feedback control was only applicable to the linear plant such that the large angle rotation have to be split as several fractions to take more control efforts. The second one is that this paper's methods have robustness to the modeling errors with the help of the passivity theorem, while the state feedback control in [14] did not hold this property explicitly.

5. Conclusions

In this paper, two output feedback control schemes are investigated to facilitate the attitude takeover control of a retired spacecraft using multiple cellular space modules. These cellular space modules are regarded as players in the attitude takeover control process formulated as a differential game, and they are classified as two types of cellular space modules, namely OCSM and RCSM. The attitude controllers include the pre-wrap control part and the rate feedback control part, designed for the OCSM and RCSM respectively. The first scheme, static output feedback, is designed using the output feedback differential-game-based control. The second scheme, dynamic output feedback, is organized as a dynamic strictly positive real compensator using the Kalman–Yakubovich–Popov Lemma, in which the controller parameter matrices are calculated from the results of state feedback differential-game-based control. Although both control schemes are designed using a linear model of the spacecraft dynamics, the use of passivity theorem guarantees that the proposed control schemes can stabilize the original nonlinear plant. These control methods are robust to the modeling errors since the stability of the closed-loop system has no hinge on the inertia information of the retired spacecraft. The effectiveness of the proposed two output feedback control schemes are demonstrated through numerical simulations. Compared with an existing method, it shows that the proposed control schemes have lower energy consumption to attain the steady state but taking a similar transient time interval as the existing method spend.

Declaration of competing interest

No competing interest.

Acknowledgment

This work is supported by the Canada Research Chairs program, Grant number 950-230883.

Appendix

Claim. *The matrix $\boldsymbol{W}_i$ shown in Eq. (52) is positive definite when the matrix $\boldsymbol{R}_{ii} = r_{ii}\boldsymbol{\varphi}_i^\top \boldsymbol{I}\boldsymbol{\varphi}_i$ where r_{ii} is a positive scalar constant.*

Proof. Recalling the definition of $\boldsymbol{W}_i$ and considering Eqs. (43)(45) gives:

$$\begin{aligned}\boldsymbol{W}_i &= \boldsymbol{R}_{ii}^{-1}\boldsymbol{B}_i^\top \boldsymbol{P}_i \boldsymbol{C}_i^\top \left(\boldsymbol{C}_i\boldsymbol{C}_i^\top\right)^{-1} \\ &= r_{ii}\boldsymbol{\varphi}_i^\top \boldsymbol{I}\boldsymbol{\varphi}_i \begin{bmatrix} \mathbf{0} \\ \boldsymbol{I}^{-1}\boldsymbol{\varphi}_i \end{bmatrix}^\top \boldsymbol{P}_i \begin{bmatrix} \mathbf{0} & \boldsymbol{\varphi}_i^\top \end{bmatrix}^\top \left(\begin{bmatrix} \mathbf{0} & \boldsymbol{\varphi}_i^\top \end{bmatrix} \begin{bmatrix} \mathbf{0} & \boldsymbol{\varphi}_i^\top \end{bmatrix}^\top \right)^{-1}\end{aligned} \tag{63}$$

Since the direction cosine matrix $\boldsymbol{\varphi}_i$ satisfies $\boldsymbol{\varphi}_i\boldsymbol{\varphi}_i^\top = \mathbf{1}$ ($\mathbf{1}$ is the identity matrix), one has that:

$$\boldsymbol{W}_i = r_{ii} \begin{bmatrix} \mathbf{0} & \boldsymbol{\varphi}_i^\top \end{bmatrix} \boldsymbol{P}_i \begin{bmatrix} \mathbf{0} \\ \boldsymbol{\varphi}_i \end{bmatrix} \tag{64}$$

The positive definite matrix $\boldsymbol{P}_i$ can be partitioned as

$$\boldsymbol{P}_i = \begin{bmatrix} \boldsymbol{P}_{i,11} & \boldsymbol{P}_{i,12} \\ \boldsymbol{P}_{i,12}^\top & \boldsymbol{P}_{i,22} \end{bmatrix} \tag{65}$$

Hence,

$$\boldsymbol{W}_i = r_{ii}\boldsymbol{\varphi}_i^\top \boldsymbol{P}_{i,22}\boldsymbol{\varphi}_i \tag{66}$$

According to Schur complement Lemma [33], $\boldsymbol{P}_i > 0 \Rightarrow \boldsymbol{P}_{i,22} > 0$. For a vector $\boldsymbol{v} \neq \mathbf{0} \in \mathbb{R}^3$, we have

$$\boldsymbol{v}^\top \boldsymbol{W}_i \boldsymbol{v} = \left(\boldsymbol{\varphi}_i\boldsymbol{v}\right)^\top \left(r_{ii}\boldsymbol{P}_{i,22}\right)\left(\boldsymbol{\varphi}_i\boldsymbol{v}\right) > 0 \tag{67}$$

which implies that $\boldsymbol{W}_i$ is positive definite. This concluded the proof.

References

[1] J. Choi, J. Jung, D. Lee, B. Kim, Articulated linkage arms based reliable capture device for janitor satellites, Acta Astronaut. 163 (2019) 91–99, http://dx.doi.org/10.1016/j.actaastro.2019.03.002.

[2] Y. Liu, Y. Zhao, C. Tan, H. Liu, Y. Liu, Economic value analysis of on-orbit servicing for geosynchronous communication satellites, Acta Astronaut. (2020) http://dx.doi.org/10.1016/j.actaastro.2020.11.040.

[3] Y. Wang, P. Gurfil, Deorbiting timing for spacecraft in geostationary transfer orbits exploiting Luni–solar perturbations, J. Spacecr. Rockets 55 (1) (2018) 251–256, http://dx.doi.org/10.2514/1.a33938.

[4] B. Meng, J. Huang, Z. Li, L. Huang, Y. Pang, X. Han, Z. Zhang, The orbit deployment strategy of OOS system for refueling near-earth orbit satellites, Acta Astronaut. 159 (2019) 486–498, http://dx.doi.org/10.1016/j.actaastro.2019.02.001.

[5] D. Barnhart, B. Sullivan, Economics of repurposing in situ retired spacecraft components, in: AIAA SPACE 2012 Conference & Exposition, 2012, p. 5304, http://dx.doi.org/10.2514/6.2012-5304.

[6] D.A. Barnhart, R. Rughani, J.J. Allam, K.W. Clarke, Initial safety posture investigations for earth regime rendezvous and proximity operations, J. Space Saf. Eng. 7 (4) (2020) 519–524, http://dx.doi.org/10.1016/j.jsse.2020.06.010.

[7] M. Goeller, J. Oberlaender, K. Uhl, A. Roennau, R. Dillmann, Modular robots for on-orbit satellite servicing, in: 2012 IEEE International Conference on Robotics and Biomimetics, ROBIO, IEEE, 2012, pp. 2018–2023.

[8] M. Kortman, S. Ruhl, J. Weise, J. Kreisel, T. Schervan, H. Schmidt, A. Dafnis, Building block based iboss approach: fully modular systems with standard interface to enhance future satellites, in: 66th International Astronautical Congress, Jersualem, Israel, 2015.

[9] P. Huang, M. Wang, Z. Meng, F. Zhang, Z. Liu, Attitude takeover control for post-capture of target spacecraft using space robot, Aerosp. Sci. Technol. 51 (2016) 171–180, http://dx.doi.org/10.1016/j.ast.2016.02.006.

[10] P. Huang, M. Wang, Z. Meng, F. Zhang, Z. Liu, H. Chang, Reconfigurable spacecraft attitude takeover control in post-capture of target by space manipulators, J. Franklin Inst. B 353 (9) (2016) 1985–2008, http://dx.doi.org/10.1016/j.jfranklin.2016.03.011.

[11] P. Huang, Y. Lu, M. Wang, Z. Meng, Y. Zhang, F. Zhang, Postcapture attitude takeover control of a partially failed spacecraft with parametric uncertainties, IEEE Trans. Autom. Sci. Eng. 16 (2) (2018) 919–930, http://dx.doi.org/10.1109/tase.2018.2875139.

[12] Z. Wang, J. Yuan, D. Che, Adaptive attitude takeover control for space non-cooperative targets with stochastic actuator faults, Optik 137 (2017) 279–290, http://dx.doi.org/10.1016/j.ijleo.2017.02.071.

[13] H. Chang, P. Huang, Y. Zhang, Z. Meng, Z. Liu, Distributed control allocation for spacecraft attitude takeover control via cellular space robot, J. Guid. Control Dyn. 41 (11) (2018) 2499–2506, http://dx.doi.org/10.2514/1.g003626.

[14] Y. Chai, J. Luo, N. Han, J. Xie, Linear quadratic differential game approach for attitude takeover control of failed spacecraft, Acta Astronaut. (2020) 142–154, http://dx.doi.org/10.1016/j.actaastro.2020.04.023.

[15] Y. Chai, J. Luo, N. Han, J. Sun, Robust event-triggered game-based attitude control for on-orbit assembly, Aerosp. Sci. Technol. (2020) 105894, http://dx.doi.org/10.1016/j.ast.2020.105894.

[16] M. Innocenti, V. Tartaglia, Game theoretic strategies for spacecraft rendezvous and motion synchronization, in: AIAA Guidance, Navigation, and Control Conference, 2016, p. 0873, http://dx.doi.org/10.2514/6.2016-0873.

[17] P. Ghorawat, K. Lee, S.N. Singh, Differential game-based control law for stabilization of aeroelastic system with gust load, in: AIAA Guidance, Navigation, and Control Conference, 2016, p. 1866, http://dx.doi.org/10.2514/6.2016-1866.

[18] D. Ye, M. Shi, Z. Sun, Satellite proximate pursuit-evasion game with different thrust configurations, Aerosp. Sci. Technol. 99 (2020) 105715, http://dx.doi.org/10.1016/j.ast.2020.105715.

[19] C.J. Damaren, Gain scheduled SPR controllers for nonlinear flexible systems, J. Dyn. Syst. Meas. Control 118 (4) (1996) 698–703, http://dx.doi.org/10.1115/1.2802345.

[20] J.R. Forbes, C.J. Damaren, Design of gain-scheduled strictly positive real controllers using numerical optimization for flexible robotic systems, J. Dyn. Syst. Meas. Control 132 (3) (2010) http://dx.doi.org/10.1115/1.4001335.

[21] A. Walsh, J.R. Forbes, A very strictly passive gain-scheduled controller: Theory and experiments, IEEE/ASME Trans. Mechatronics 21 (6) (2016) 2817–2826, http://dx.doi.org/10.1109/tmech.2016.2565387.

[22] A. Walsh, J.R. Forbes, Analysis and synthesis of input strictly passive gain-scheduled controllers, J. Franklin Inst. B 354 (3) (2017) 1285–1301, http://dx.doi.org/10.1016/j.jfranklin.2016.03.014.

[23] J. Jang, A. Lee, N. Bedrossian, P. Spanos, Design of robust Nash game theoretic controllers with time domain constraints, in: Proceedings of the 2003 American Control Conference, 2003, Vol. 6, IEEE, 2003, pp. 5363–5368, http://dx.doi.org/10.1109/acc.2003.1242581.

[24] K.G. Vamvoudakis, F.L. Lewis, Multi-player non-zero-sum games: Online adaptive learning solution of coupled Hamilton–Jacobi equations, Automatica 47 (8) (2011) 1556–1569, http://dx.doi.org/10.1016/j.automatica.2011.03.005.

[25] T. Li, Z. Gajic, Lyapunov Iterations for solving coupled algebraic riccati equations of Nash differential games and algebraic riccati equations of zero-sum games, in: New Trends in Dynamic Games and Applications, Springer, 1995, pp. 333–351.

[26] H.J. Marquez, Nonlinear Control Systems: Analysis and Design, John Wiley & Sons, Inc., New Jersey, 2002.

[27] J.T. Wen, Time domain and frequency domain conditions for strict positive realness, IEEE Trans. Automat. Control 33 (10) (1988) 988–992, http://dx.doi.org/10.1109/9.7263.

[28] P.C. Hughes, Spacecraft Attitude Dynamics, Dover Publications, Mineola, New York, 2004.
[29] J.R. Forbes, Passivity-based attitude control on the special orthogonal group of rigid-body rotations, J. Guid. Control Dyn. 36 (6) (2013) 1596–1605, http://dx.doi.org/10.2514/1.59270.
[30] K.J. Jensen, Generalized nonlinear complementary attitude filter, J. Guid. Control Dyn. 34 (5) (2011) 1588–1593, http://dx.doi.org/10.2514/1.53467.
[31] F. Lizarralde, J.T. Wen, Attitude control without angular velocity measurement: A passivity approach, IEEE Trans. Automat. Control 41 (3) (1996) 468–472, http://dx.doi.org/10.1109/9.486654.
[32] J. Engwerda, A. Weeren, A result on output feedback linear quadratic control, Automatica 44 (1) (2008) 265–271, http://dx.doi.org/10.1016/j.automatica.2007.04.025.
[33] G. Duan, H. Yu, LMIs in Control Systems: Analysis, Design and Applications, CRC Press, 2013.